Toward an Augmented Target-Controlled Infusion System for an Automated Anesthesia with Hypnosis and Analgesia Objectives*

Pablo S. Rivadeneira[1,2], Jérôme Cieslak[2], Ariana Gutiérrez[2], David Gucik-Derigny[2], David Henry[2], Agnès Drochon[3], Claire Oddos[4], Lucas Martin[4], Bogdan Catargi[5] and Alexandre Ouattara[4,6]

***Abstract*— For major surgery, Target-controlled infusion (TCI) systems are currently the gold standard to achieve safe anesthesia. Based on pharmacokinetic (PK) and pharmacodynamic (PD) models, the TCI system administers the necessary amount of drugs to achieve clinical targets, but does not account for drug interactions or surgical disturbances, such as incisions or skin manipulation. To overcome these weaknesses, the integration of an augmented intelligence into the TCI system is proposed. First, the effect of surgical stimuli, as reflected in the outputs, is estimated. Next, an adaptation mechanism is introduced to smoothly mitigate the impact of disturbances and achieve clinical targets for depth of hypnosis and analgesia. The benefits of the proposed solution are finally highlighted by using the AReS simulator as a substitute for pre-clinical testing.**

I. INTRODUCTION

To address the dual challenges of an aging population and rising rates of chronic disease, the integration of automation into healthcare organizations is increasingly accepted. Among the current solutions, the Target-controlled infusion (TCI) systems are currently the gold standard to achieve safe anesthesia in Total Intravenous Anesthesia (TIVA) road [1], paving the way for a transformation in patient care to reduce clinical staff workload. More precisely, the TCI system comprises predictive algorithms and pumps for drug administration. Moreover, TIVA is a common surgical procedure that aims to simultaneously maintain hypnosis, analgesia, neuromuscular blockade, and hemodynamic stability through continuous infusion of drugs such as propofol, remifentanil, rocuronium, and norepinephrine. From a control perspective, TIVA is inherently multivariable, nonlinear, subject to inter- and intra-patient variability, surgical stimuli effects (disturbances), and interactions of the pharmacological agents.

Pharmacokinetic–pharmacodynamic (PK/PD) models have provided a quantitative description of medication effects and led to the development of TCI systems. TCI-guided anesthesia has led to better regulation of physiological effects during surgery and, in consequence, improved postoperative recovery [2]. According to [3], the TCI system is a pure feed-forward open-loop strategy, operating in a "virtual" closed-loop configuration, *i.e.*, TCI unit adapts the intravenous drug infusion rate to achieve a desired target concentration in the shortest possible time, without using available physiological measurements, accounting for drug interactions or surgical stimuli [4]. Although more precise than manual control, it is always the anesthetist's responsibility to adapt drug infusions based on several physiological measurements, which can involve a heavy workload for clinical staff [2].

In the surgical room, the typical available measurements are the bispectral index (BIS) linked to the depth of hypnosis (DOH), the train-of-four for the neuromuscular blockade (NMB), the mean arterial pressure, the stroke volume, the cardiac output, and the heart rate for the assessment of the hemodynamic stability. For the nociception monitoring, several monitors have been developed, such as the surgical pleth index (SPI), but none of them is a gold standard yet [5]. To take advantage of this available information and provide a faster response, automatic closed-loop control systems have been developed [6] to adjust drug infusions in real time based on continuous physiological measurements, thereby improving performance, enabling faster reaction than manual systems, and reducing the anesthesiologist's workload. In this context, several techniques have been proposed, such as proportional, integral, and derivative (PID) control [7], model predictive control (MPC) [8], and robust control [9], to name a few. However, there are no commercial devices that implement these solutions, and even if some results have already crossed the translational research threshold [6], the clinical acceptability of these solutions remains fragile.

Taking this into consideration, recent proposals attempt to improve the actual TCI systems, mainly proposing it for other drugs (e.g., in [10], a state-feedback design method for the automatic control of the NMB is designed and converted to a TCI for rocuronium), or trying to modify the actual algorithm to improve performance. An interesting proposal is presented in [4] where the interaction target-controlled infusion (iTCI) is introduced. This system uses the combined PK/PD model of propofol and remifentanil to reduce the drug quantity required by the standard TCI. However, the targets are not updated when surgical stimuli affect the patient, leading to increased DOH and reduced analgesia.

In this context, the first paper contribution is adapted

* This study has received financial support from the French government in the framework of the France 2030 programme IdEx Université de Bordeaux and the 2025 Visiting Scholar campaign of the University of Bordeaux. [1]Universidad Nacional de Colombia, Facultad de Minas, Departamento de Energía Eléctrica y Automática, Grupo GITA, Cra. 80 # 65 – 223, Medellin, Colombia psrivade@unal.edu.co. [2]Univ. Bordeaux, CNRS, Bordeaux INP, IMS,UMR 5218, F-33400, Talence, France. (jerome.cieslak, david.gucik-derigny, david.henry)@ims-bordeaux.fr. [3]Univ. Bordeaux, CNRS, Bordeaux INP, I2M, UMR 5295, F-33400, Talence, France. agnes.drochon@u-bordeaux.fr. [4]CHU Bordeaux, Dpt of Cardiovascular Anesthesia and Critical Care, 33000, Bordeaux, France. (claire.oddos, lucas.martin)@chu-bordeaux.fr. [5]Hôpital Saint-André, Dpt of Endocrinology and Metabolic Diseases, 33000, Bordeaux. bogdan.catargi@chu-bordeaux.fr. [6]Univ. Bordeaux, INSERM, 1034, Biology of Cardiovascular Diseases, 33600, Pessac. alexandre.ouattara@chu-bordeaux.fr

from the fault hiding paradigm [11] – this concept aims to introduce a reconfiguration block, known as virtual actuators, for the actuator failure case, that hides the presence of the fault from the baseline controller [12] –, *i.e.*, it is proposed to integrate the virtual surgical effect estimation between the effect-site target computation and the baseline TCI system. To update the target, an extended Kalman filter (EKF) augmented with a disturbance model is designed to produce state and disturbance estimates. Based on this estimate, a correction target factor is computed using a proportional rule, with hard constraints to limit the maximum allowed change and prevent overdosage. The second contribution concerns the inclusion of the SPI monitor to guide remifentanil infusion. Thus, the TCI system targets the computation of propofol and remifentanil control signals, obtained using a novel PD equation for SPI and a surface equation for BIS, accounting for drug interactions, and is updated using specific disturbance estimates affecting BIS and SPI. Finally, the performance of the proposed TCI system is assessed *in silico* using a 44-patient cohort in the AReS simulator, demonstrating that the new system maintains BIS and SPI within the desired ranges even under surgical stimuli.

II. Preliminaries

A. Virtual human for anesthesia

The infusion rates of propofol and remifentanil are considered as system inputs. In the literature, several three-compartment pharmacokinetic models for propofol and remifentanil have been reported to describe drug distribution in the body. The most common is the Schnider model for propofol [13] and the Minto model for remifentanil [14]. However, the most up–to–date and comprehensive model covering a large population is the Eleveld model for both drugs [15], [16]. The PK model for both drugs can be expressed as

$$\dot{\mathbf{x}}_m(t) = A_m\mathbf{x}(t) + B_m u_m(t), \quad \mathbf{x}_m(0) = \mathbf{x}_{m0}, \tag{1}$$

with

$$A_m = \begin{pmatrix} -(a_{10m}+a_{12m}+a_{13m}) & a_{21m} & a_{31m} \\ a_{12m} & -a_{21m} & 0 \\ a_{13m} & 0 & -a_{31m} \end{pmatrix},$$
$$B_m = \begin{pmatrix} \frac{1}{V_{1m}} \\ 0 \\ 0 \end{pmatrix}, \tag{2}$$

where the index m can be p or r associated to propofol and remifentanil, $\mathbf{x}_m$ stands for the state vector $\mathbf{x}_m = (x_{1,m}\ \ x_{2,m}\ \ x_{3,m})^\top$, and $x_{1,m}$ is the plasma drug concentration, while $x_{2,m}$, and $x_{3,m}$ are the respective drug concentration in fast and slow compartments. The initial condition is $\mathbf{x}_{m0} \in \mathbb{R}^3$, and $u_m \in \mathbb{R}$ is the intravenous infusion rate of the drug m. The constants a_{ij}, with $i, j = 1, 2, 3$, and $i \neq j$, represent the drug amount transfer rate from the i–th compartment to the j–th compartment, are given as follows

$$a_{10m} = \frac{Cl_{1m}}{V_{1m}},\ a_{12m} = \frac{Cl_{2m}}{V_{1m}},\ a_{13m} = \frac{Cl_{3m}}{V_{1m}},$$
$$a_{21m} = \frac{Cl_{2m}}{V_{2m}},\ a_{31m} = \frac{Cl_{3m}}{V_{3m}}, \tag{3}$$

where V_{im}, for $i = 1, 2, 3$, denotes the volume of the i–th compartment of the drug m, and Cl_{im} represents its corresponding clearance rate. These parameters depend on demographic information (such as age, weight, height, body mass index, sex) and are given in Appendices V-A and V-B. The PD model comprises both linear and nonlinear components. The linear component describes the relationship between drug plasma concentration, $x_{1,m}$, and its effect–site concentration, $x_{4,m}$. The linear part of the PD model for propofol and remifentanil is

$$\dot{x}_{4,m}(t) = k_{1e}x_{1,m}(t) - k_{e0}x_{4,m}(t), \tag{4}$$

where k_{e0} and k_{1e} are the drug metabolic rate constants. The nonlinear component defines the relationship between the effect-site concentration and the clinical or physiological effect. This is typically modeled with a "Hill" function.

Two system outputs are considered in this work: DOH (linked to the BIS monitor) and analgesia level (obtained by the SPI monitor). The BIS monitor is the most common practice in surgical rooms. BIS correlates not only with hypnotic drugs, but also with opioids. The so-called surface equation, which is an extended Hill function when there is a drug interaction, is used here [17] according to

$$BIS = BIS_0 - BIS_{\max}\left(\frac{\left(\frac{U_p+U_r}{U_{50}(\phi)}\right)^\gamma}{1+\left(\frac{U_p+U_r}{U_{50}(\phi)}\right)^\gamma}\right) = h_1(\mathbf{x}_4), \tag{5}$$

with

$$U_p(t) = \frac{x_{4,p}(t)}{EC_{50,p}},\ U_r(t) = \frac{x_{4,r}(t)}{EC_{50,r}}, \tag{6}$$
$$\phi(t) = \frac{U_p(t)}{U_p(t)+U_r(t)},\quad U_{50}(\phi(t)) = 1 - \beta\phi(t) + \beta\phi^2(t),$$

where U_p and U_r are normalized effect–site concentrations of propofol and remifentanil, and ϕ is a dimensionless parameter that represents the combined effect of propofol and remifentanil. $EC_{50,p}$ and $EC_{50,r}$ are the the effect–site concentration values associated with half the difference of BIS_0 and BIS_{max} for propofol and remifentanil. U_{50} is the term required for the normalization of the drug combined effect, where β is the synergistic effect taken as $\beta = 1$. The parameters BIS_0 and BIS_{max} are taken as equal [18].

As described in the literature, direct measurements of nociception are not available, but several indirect indicators have been developed to indicate nociceptive stimuli during surgery [19], [20]. In this work, particular attention is given to SPI since it can be easily computed using photoplethysmographic signals in the clinical setting as $SPI(t) = 100 - (0.3HBI_{norm}(t) + 0.7PPGA_{norm}(t))$, where HBI_{norm} is the normalized heartbeat interval and $PPGA_{norm}$ is

TABLE I

OUTPUT TARGET VALUES AND SAFETY RANGES.

Outputs	Targets	Normal Range	Risky Range
BIS (%)	50	40–60	<40, >60
SPI (%)	38	25–50	<25, >50

TABLE II

PLASMA CONCENTRATION AND INFUSION RATE LIMITS [25].

Drug	Propofol	Remifentanil
Plasma concentration constraint	0-10 μg/mL	0-10 ng/mL
Infusion rate constraint	0-2 mg/s	0-0.5 μg/s

the normalized waveform amplitude [19]. A PD model is proposed here for SPI as a function mainly of remifentanil [21], namely

$$SPI = SPI_{max}\left(1 - \frac{x_{4,m}^{\gamma_{SPI}}(t)}{x_{4,m}^{\gamma_{SPI}}(t) + EC_{50,SPI}^{\gamma_{SPI}}}\right) = h_2(x_{4,r}), \quad (7)$$

where $SPI_{\max} = 80$ is the maximum reachable effect by means of the drug administration and taken from the clinical studies in [22], $EC_{50,SPI} = 2.41$ ng/ml corresponds to the effect–site concentration associated with half the difference of $SPI_{\max}$ and was computed to obtain the same probability of no response described in [23], and $\gamma_{SPI} = 0.72$ taken from [17] is the steepness of the sigmoidal relationship.

B. TCI description

The computerized system running in modern TCI pumps employs a numerical closed-form algorithm to calculate the infusion rate necessary to achieve and maintain any desired concentration at the site of drug action as rapidly as possible, without overshoot, based on an internal model [24]. Mathematically, this problem can be stated as an optimal control [4]

$$\begin{aligned} u_m(t) \quad &= \quad \arg\min_{t_f, u_m} t_f \\ \text{s.t.} \quad & \\ & \dot{\mathbf{x}}_m(t) = A_m \mathbf{x}_m(t) + B_m u_m(t), \\ & x_{4,m}(t_f) = x_{4,m}^{TCI} \\ & 0 \le u_m(t) \le u_m^{max}. \end{aligned} \quad (8)$$

where t_f is the final time to reach the target, $x_{4,m}^{TCI}$ is the desired target to configure in the TCI pump, and u_m^{max} is the maximum allowed infusion rate. A discretized version of this algorithm is included in the AReS simulator, where the internal model for propofol and remifentanil can be selected from the available types described in the previous subsection.

III. PROPOSED SCHEME

Additional systems based on virtual disturbance estimation are proposed to improve the adaptability of TCI systems in the operating room, see green lines in Fig. 1. The patient is simulated using a combination of PK and PD models described in section II. The TCI system computes the necessary infusion rates by using the predefined effect-site (ES) concentrations ($\mathbf{x}_4^{TCI} = (x_{4,p}^{TCI} \quad x_{4,r}^{TCI})^\top$) of both drugs as targets, as specified by the block 'TCI algorithm'. The virtual patient and the TCI block are provided by the AReS simulator [18].

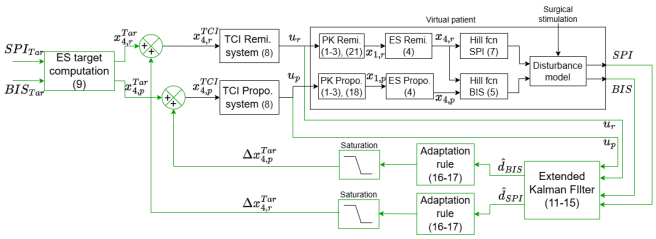

Fig. 1. Proposed scheme setup: The virtual patient and the actual TCI system are drawn in black, and the proposed scheme is highlighted in green.

A. Integrating drug interaction and SPI measurement

In current practice, the ES targets for propofol and remifentanil are set by the anesthesiologists. Here, it is proposed to compute them by using output targets (BIS_{Tar} and SPI_{Tar}). Following the idea introduced by [4], the effect-site propofol and remifentanil targets, $\mathbf{x}_4^{Tar}$, are calculated using the interaction equation (5) and (7) to avoid the need for the ratio and profit from the information of the SPI measurement. The recommended SPI target to achieve adequate analgesia is $SPI < 40$ [5]. Therefore, the SPI target was set at 37, whereas the recommended BIS target to maintain an adequate DOH is typically 50. Then, the TCI target solves the problem:

$$\begin{aligned} \mathbf{x}_4^{Tar} = \{(x_{4,p}, x_{4,r}) \quad | \quad & BIS_{Tar} - h_1(\mathbf{x}_4) = 0 \quad \& \\ & SPI_{Tar} - h_2(x_{4,r}) = 0\}. \end{aligned} \quad (9)$$

when the extra system is deactivated, $\mathbf{x}_4^{Tar} = \mathbf{x}_4^{TCI}$ is satisfied. In Tables I and II, the output normal ranges, risky ranges, targets, and infusion limits are described.

B. Surgical effect estimation

To compute the correction term $\Delta\mathbf{x}_4^{Tar} = (\Delta x_{4,p}^{Tar} \quad \Delta x_{4,r}^{Tar})^\top$ of the target $\mathbf{x}_4^{Tar} = (x_{4,p}^{Tar} \quad x_{4,r}^{Tar})^\top$, an estimation setup is considered in which the state ($\hat{\mathbf{x}}$) and disturbance ($\hat{\mathbf{d}}$) are estimated. The nonlinear observability criterion was evaluated through the Lie derivatives [26], and its rank was 10, allowing us to estimate the state and the disturbance. If only the BIS output is selected, the 8 states and 1 disturbance can be estimated. However, if SPI is selected alone, only the state related to remifentanil can be estimated, and its corresponding disturbance.

To be able to jointly estimate the state vector and the surgical disturbance vector, the concept of the extended

Kalman filter (EKF) is used, i.e., the augmented model is

$$\begin{pmatrix} \mathbf{x}(k) \\ \mathbf{d}(k) \end{pmatrix} = \underbrace{\begin{pmatrix} A_d & M_e \\ 0_{2\times 8} & I_{2\times 2} \end{pmatrix}}_{A^{ext}} \begin{pmatrix} \mathbf{x}(k-1) \\ \mathbf{d}(k-1) \end{pmatrix} + \underbrace{\begin{pmatrix} B_d \\ 0_{2\times 1} \end{pmatrix}}_{B^{ext}} \mathbf{u}(k-1) + G_w \mathbf{w}(k-1), \quad (10)$$

$$\mathbf{y}(k) = \mathbf{h}(\mathbf{x}(k)) + \mathbf{d}(k) + \mathbf{v}(k),$$

where $\mathbf{x} = [\mathbf{x}_p \ \ \mathbf{x}_r]^\top \in \mathbb{R}^8$ is the state associated to propofol and remifentanil, $\mathbf{u} = [u_p \ \ u_r]^\top$ is the input, $\mathbf{y}$ is the output, $\mathbf{h} = (h_1 \ h_2)^\top$ is defined with the Eq. (5) for BIS and with Eq. (7) for SPI, $\mathbf{d}$ are the disturbance augmented states for BIS and SPI, A_d and B_d represent the discrete versions of $A = \text{diag}(A_p, A_r)$ and $B = \text{diag}(B_p, B_r)$, respectively. The matrix $M_e = \begin{pmatrix} 0 & 0 & 0 & 1 & 0 & 0 & 0 & 0 & 0 & 0 \\ 0 & 0 & 0 & 0 & 0 & 0 & 0 & 1 & 0 & 0 \end{pmatrix}^T$, G_w is a matrix affecting only the plasma and effect–site concentrations, $\mathbf{w}(k) \in \mathbb{R}$ is assumed to be a zero-mean Gaussian process noise, with variance Q^{ext}, and $\mathbf{v}(k) \in \mathbb{R}^2$ is assumed to be a zero-mean Gaussian output noise with variance R^{ext}. The value of R^{ext} should be computed according to the variance of the BIS and SPI measurements, while the value of Q^{ext} is used as a tuning parameter for the estimation performance. Roughly speaking, a large Q^{ext}/R^{ext} ratio is selected when the measurement is confident. In contrast, a small Q^{ext}/R^{ext} ratio is selected when the measurement noise is high, and the model is accurate. The EKF is implemented with the following recursion

$$\hat{\mathbf{x}}_k^- = A_{ext}\hat{\mathbf{x}}_k + B_{ext}\mathbf{u}_k, \quad H_k = \left.\frac{\partial \mathbf{h}(\mathbf{x})}{\partial \mathbf{x}}\right|_{\hat{\mathbf{x}}_k}, \quad (11)$$

$$P_k^- = A_{ext}P_{k-1}A_{ext}^\top + G_w Q^{ext} G_w^\top, \quad (12)$$

$$L_k = P_j^- H_k^\top (H_k P_k^- H_k^\top + R^{ext})^{-1}, \quad (13)$$

$$\hat{\mathbf{x}}_k = \hat{\mathbf{x}}_k^- + L_k(\mathbf{y}_k - \hat{\mathbf{y}}(\hat{\mathbf{x}})), \quad (14)$$

$$P_k = (I - L_k H_k)P_k^-. \quad (15)$$

where $P_0 = I$ has the appropriate dimensions. I denotes the identity matrix, and, abusing on notation, $\hat{\mathbf{x}}$ stands for the estimated state and disturbance.

C. Adaptation rule

Once the state and the disturbance are estimated, it is proposed to use the virtual disturbance to modify the target to the TCI systems, especially to counteract external disturbance effects. Here, a proportional rule is chosen to assess its ability to provide improved DOH and analgesia levels. The proposed adaptation rule is

$$\mathbf{x}_4^{TCI} = \mathbf{x}_4^{Tar} + \min(\Delta \mathbf{x}_4^{Tar}, \mathbf{Th}), \quad (16)$$

$$\Delta \mathbf{x}_4^{Tar} = K\hat{\mathbf{d}}, \quad K = \begin{pmatrix} \frac{1}{d_{p,max}} & 0 \\ 0 & \frac{1}{d_{r,max}} \end{pmatrix}. \quad (17)$$

The gain $\mathbf{d}_{max} = [12 \ 10]^\top$ and $\mathbf{Th} = [0.7 \ 0.9]^\top$ were tuned by trial and error to achieve an adequate level of DOH and analgesia, *i.e.*, around the output targets.

IV. Results and discussion

The proposed augmented TCI system is assessed using the AReS Simulator with a population of 44 virtual human patients [18], in which the analgesia dynamics described by Eq. (7) and necessary parameters for integrating SPI were added. AReS simulator has also incorporated inter-individual variability and surgical disturbances, including intubation, incision, skin and suture manipulations, and hypovolemia.

Simulations were run on a workstation with a Windows 10 64-bit operating system, 64 GB of RAM, and an Intel(R) Xeon(R) W-10855M CPU @ 2.80GHz 2.81 GHz processor. The sampling time was 5 seconds, and the total simulation time was 35 minutes. The estimator parameters were tuned to $Q_{ext} = \text{diag}[0.01 \ 0.01 \ 0.01 \ 0.01 \ 0.03 \ 0.01 \ 0.01 \ 0.01 \ 1 \times 10^3 \ 1 \times 10^3]$, $R_{ext} = \text{diag}[0.05 \ 0.003]$ by trial and error. The simulated surgery scenario is composed of two parts:

i) Induction phase: The first five minutes are dedicated to this phase (illustrated with a light blue patch in the figures). During this period, the control objective is to achieve the target set on the BIS output (50%), ensuring adequate DOH prior to surgical manipulation. Moreover, one disturbance is included in this phase: 1) *Intubation:* from minute 1 to minute 3 (duration 2 minutes).

ii) Maintenance phase: During this phase, the objective is to attenuate the effect of external and internal disturbances in the anesthetic and analgesic variables. The following clinical stimuli (disturbances) are included:

2) *Incision:* from minute 7 to minute 9.
3) *Skin manipulation:* from minute 11 to minute 26.
4) *Suture procedure:* from minute 27 to minute 32.
5) *Hypovolemic state:* from minute 9 to minute 23.

The last consideration in the simulation was that no manual adjustment was included when disturbances were present to highlight the difference with our proposal. To assess the performance of the proposed TCI system against the standard one, several metrics were computed. Only the time required to reach the BIS at 60% (TT) is included for the induction phase, while for the maintenance phase, the following are used: the maximum value (HV) and minimum value (LV) for each output, and the percentage of time the outputs remain within their prescribed clinical ranges (%TCR). In addition, the total drug administered was included for both phases.

In this comparison, the target $\mathbf{x}_4^{TCI}$ coincides with $\mathbf{x}_4^{Tar}$ for the TCI system alone and is adjusted (as the PK model) for each patient based on demographic information and the Eleveld model (see the Appendix).

In Fig. 2, the outputs BIS and SPI for both strategies are shown. The TCI system is depicted in red, and the augmented system in black. In the first case, the BIS remained around 65, with a maximum of 80, indicating that the anesthesiologist must act to prevent this from requiring ongoing attention. With the augmented strategy, BIS was kept around 50, and 90% of the time was in the 40-60 range after the induction time, suggesting less anesthesiologist attention. Similarly, the SPI is maintained in adequate analgesia with the augmented TCI system and insufficient most of the time

with the standard TCI system without manual adjustments.

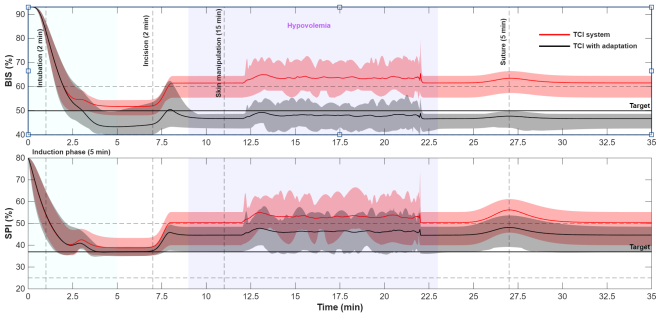

Fig. 2. BIS and SPI measurements for both strategies under disturbances.

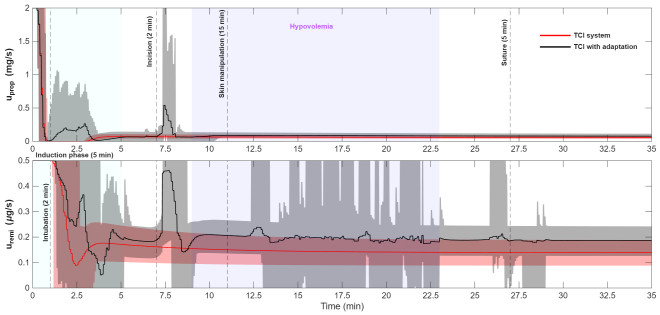

Fig. 3. Infusion rates for both strategies under disturbances.

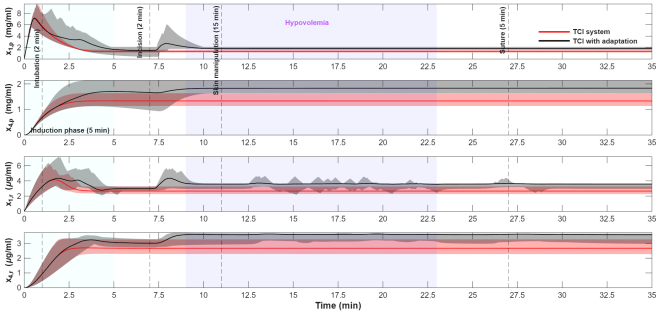

Fig. 4. Estimated plasma and effect-site concentration under disturbances.

In Fig. 3, the infusion rates are plotted. It is clear that the impact of the virtual disturbance estimation (plotted in Fig 5) and the adaptation rule, especially with the remifentanil, is significant. More drug quantity is administered with our proposal, but it is expected to counteract the disturbances. Moreover, the strategy satisfactorily rejects disturbances while respecting the input constraints.

In Fig. 4, the estimated plasma and effect-site concentration for propofol and remifentanil are shown. These variables are affected, especially during disturbances. However, in the propofol case, the variation of $\hat{x}_{1,p}$ is under the constraint of 10 mg/ml [9]. A large change is observed in remifentanil, which is expected because of the interaction between drugs, where an increase in remifentanil reduces the need for propofol, but still inside the clinically safe ranges [22].

Finally, several metrics are presented in Table III to assess the results. It is evident that the standard TCI system

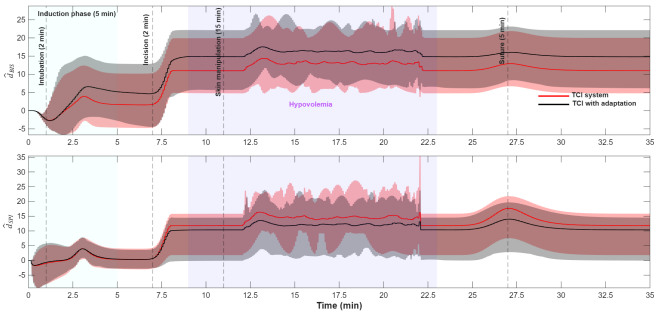

Fig. 5. Virtual disturbance estimated for both outputs, *i.e.*, BIS and SPI.

TABLE III
PERFORMANCE METRICS FOR BIS AND SPI.

Index (mean ± std)	**Standard TCI**	**Proposed scheme**
BIS		
TT (sec) (induct.)	2.03 ± 0.25	2.03 ± 0.27
LV (maint.)	51.79 ± 1.51	42.49 ± 2.18
HV (maint.)	69.79 ± 3.57	60.24 ± 0.35
TCR % (maint.)	28.75 ± 27.48	97.81 ± 1.94
SPI		
LV (maint.)	38.78 ± 2.27	36.59 ± 1.12
HV (maint.)	60.83 ± 3.96	51.46 ± 3.84
TCR % (maint.)	40.23 ± 32.70	94.70 ± 5.74
Total drug administered		
Propofol (mg)	194.83 ± 42.78	262.92 ± 55.09
Remifentanil (μg)	384.66 ± 64.30	505.32 ± 78.39

generally performs worse, but it must be noted that no anesthesiologist intervention was simulated. The proposed TCI system can respond to and handle deviations in BIS and SPI due to disturbances by administering a larger drug quantity. The output most affected by disturbances was BIS, which showed inadequate DOH levels for several patients. However, with the small adjustments performed by the proposed TCI system, it was possible to deliver adequate DOH for all patients during the disturbances, which is promising.

V. CONCLUSIONS

In this paper, the TCI system used to deliver medications during surgery is explored. The TCI system operates with predefined targets set by the anesthesiologist and must be adjusted when the professional deems it necessary, especially when surgical stimuli affect the DOH and the level of analgesia, which can be difficult. Considering this and given that the TCI system is well-accepted by clinicians, an additional system to the TCI is proposed here to automatically adjust the TCI target to maintain the outputs within the desired range. This is made possible by state and virtual disturbance estimation. Although the proposal achieves an important improvement over a constant TCI target, it requires further investigation. Specifically, other adaptation rules in magnitude and frequency can be tested.

APPENDIX

A. Parameters for the PK model for Propofol

In order to compute the constants given as in (II-A), the volumes $V_{i,p}$ (L) and their clearance rates $Cl_{i,p}$ (L/min) are

given in [15] as follows:

$$
\begin{aligned}
Cl_{1,p} &= e^{-0.0029\text{age}}\text{weight}^{0.75}\left(\frac{c_c(52\text{age}+40)^{9.06}}{(52\text{age}+40)^{9.06}+42.3^{9.06}}\right)\\
Cl_{2,p} &= 0.154V_2^{0.75}\left(1+1.3\left(1-\frac{52\text{age}+40}{52\text{age}+40+68.3}\right)\right)\\
Cl_{3,p} &= 0.0171V_3^{0.75}\left(\frac{52\text{age}+40}{52\text{age}+40+68.3}\right)\\
V_{1,p} &= 9.294\left(\frac{\text{weight}}{\text{weight}+33.6}\right)\\
V_{2,p} &= 0.364(\text{weight})e^{-0.0156(\text{age}-35)}\\
V_{3,p} &= 5.006e^{-0.0138\text{age}}(\text{FFM})
\end{aligned}
\tag{18}
$$

where $c_c = 0.0739$ for males and $c_c = 0.0868$ for females, and the fat-free mass (FFM) is computed as

$$
\text{FFM}=\left(0.88+\frac{1-0.88}{1+\left(\frac{\text{age}}{13.4}\right)^{-12.7}}\right)\left(\frac{9270\text{weight}}{6680+216\text{BMI}}\right), \tag{19}
$$

$$
\text{FFM}=\left(1.11+\frac{1-1.11}{1+\left(\frac{\text{age}}{7.1}\right)^{-1.1}}\right)\left(\frac{9270\text{weight}}{8780+246\text{BMI}}\right), \tag{20}
$$

for male and female patients, respectively. The body mass index is calculated by $\text{BMI} = \text{weight}/(\text{height}/100)^2$.

B. Parameters for the PK model for Remifentanil

The volumes $V_{i,r}$ (L) and their clearance rates $Cl_{i,r}$ (L/min) according to [16] are given as follows:

$$
\begin{aligned}
Cl_{1,r} &= 0.139(\text{FFM})^{0.75}K_{sex}e^{-0.00327(\text{age}-35)},\\
Cl_{2,r} &= 0.336K_{sex}V_2^{0.75}e^{-0.00554(\text{age}-35)},\\
Cl_{3,r} &= 0.0369V_3^{0.75}e^{-0.00554(\text{age}-35)},\\
V_{1,r} &= 0.107(\text{FFM})e^{-0.00554(\text{age}-35)},\\
V_{2,r} &= 0.162(\text{FFM})K_{sex}e^{-0.00327(\text{age}-35)},\\
V_{3,r} &= 0.0923(\text{FFM})e^{-0.0315(\text{age}-35)}e^{-0.026(\text{weight}-70)},
\end{aligned}
\tag{21}
$$

where FFM is the fat-free mass as defined before. K_{sex} for males patients is given as $K_{sex} = 1$, and for female as

$$
K_{sex} = 1+0.470\left(\frac{\text{age}^6}{\text{age}^6+12^6}\right)\left(1-\frac{\text{age}^6}{\text{age}^6+45^6}\right). \tag{22}
$$

REFERENCES

[1] P. U. Bidkar, A. Dey, P. Chatterjee, R. Ramadurai, and J. J. Joy, "Target-controlled infusion – past, present, and future," *Journal of Anaesthesiology Clinical Pharmacology*, vol. 40, no. 3, 2024.

[2] P. Šafránková and J. Bruthans, "Target-controlled infusion of propofol: A systematic review of recent results," *Journal of Medical Systems*, vol. 49, no. 1, p. 54, Apr 2025.

[3] Y. Wahlquist, A. Gustafsson, and K. Soltesz, "Exploring the influence of patient variability on propofol target-controlled infusion performance," in *2024 European Control Conference (ECC)*, 2024, pp. 3027–3032.

[4] P. Martinez-Vazquez and A. Abad-Torrent, "Simultaneous pharmacometric control optimization for advanced integrated multi-drug target infusions," *Biomedical Signal Processing and Control*, vol. 110, p. 108271, 2025.

[5] S. K. Oh, Y. J. Won, and B. G. Lim, "Surgical pleth index monitoring in perioperative pain management: usefulness and limitations," *Korean Journal of Anesthesiology*, vol. 77, no. 1, pp. 31–45, 2024.

[6] S. Coeckelenbergh, S. Boelefahr, B. Alexander, *et al.*, "Closed-loop anesthesia: foundations and applications in contemporary perioperative medicine," *Journal of Clinical Monitoring and Computing*, vol. 38, pp. 487–504, 2024.

[7] F. Padula, C. Ionescu, N. Latronico, M. Paltenghi, *et al.*, "Optimized PID control of depth of hypnosis in anesthesia," *Computer methods and programs in biomedicine*, vol. 144, pp. 21–35, 2017.

[8] A. Pawłowski, M. Schiavo, N. Latronico, M. Paltenghi, and A. Visioli, "Model predictive control using miso approach for drug coadministration in anesthesia," *Journal of Process Control*, vol. 117, pp. 98–111, 2022.

[9] G. A. Dumont, A. Martinez, and J. M. Ansermino, "Robust control of depth of anesthesia," *International Journal of Adaptive Control and Signal Processing*, vol. 23, no. 5, pp. 435–454, 2009.

[10] J. Silva, T. Mendonça, and P. Rocha, "Improving tci control for the automatic delivery of rocuronium," in *2020 28th Mediterranean Conference on Control and Automation (MED)*, 2020, pp. 905–908.

[11] J. Lunze and T. Steffen, "Control reconfiguration after actuator failures using disturbance decoupling methods," *IEEE Transactions on Automatic Control*, vol. 51, no. 10, pp. 1590–1601, 2006.

[12] J. Cieslak and D. Henry, "A switching fault-hiding mechanism based on virtual actuators and dwell-time conditions," *IFAC-PapersOnLine*, vol. 51, no. 24, pp. 703–708, 2018.

[13] T. W. Schnider, C. F. Minto, P. Cambus, *et al.*, "The influence of method of administration and covariates on the pharmacokinetics of propofol in adult volunteers," *Anesthesiology*, vol. 88, pp. 1170–1182, 1998.

[14] C. F. Minto, M. White, N. Morton, and G. N. Kenny, "Pharmacokinetics and pharmacodynamics of remifentanil, ii. model application," *Anesthesiology*, vol. 86, no. 1, pp. 24–33, 1997.

[15] D. J. Eleveld, P. Colin, A. R. Absalom, and M. M. Struys, "Pharmacokinetic–pharmacodynamic model for propofol for broad application in anaesthesia and sedation," *British journal of anaesthesia*, vol. 120, no. 5, pp. 942–959, 2018.

[16] D. J. Eleveld, J. H. Proost, H. Vereecke, A. R. Absalom, *et al.*, "An allometric model of remifentanil pharmacokinetics and pharmacodynamics," *Anesthesiology*, vol. 126, no. 6, pp. 1005–1018, 2017.

[17] T. W. Bouillon, . Bruhn, J, L. Radulescu, C. Andresen, *et al.*, "Pharmacodynamic interaction between propofol and remifentanil regarding hypnosis, tolerance of laryngoscopy, bispectral index, and electroencephalographic approximate entropy." *Anesthesiology*, vol. 100, no. 6, pp. 1353–1372, 2004.

[18] S. Hosseinirad, M. Merlo, F. Trovò, E. Tognoli, A. M. Metelli, and G. A. Dumont, "Ares: A patient simulator to facilitate testing of automated anesthesia," *Computer Methods and Programs in Biomedicine*, vol. 269, p. 108901, 2025.

[19] M. Huiku, K. Uutela, M. Van Gils, I. Korhonen, *et al.*, "Assessment of surgical stress during general anaesthesia," *British journal of anaesthesia*, vol. 98, no. 4, pp. 447–455, 2007.

[20] P. Laferriere-Lanlgois, L. Morisson, S. Jeffries, *et al.*, "Depth of anesthesia and nociception monitoring: Current state and vision for 2050," *Anesthesia & Analgesia*, vol. 138, no. 2, pp. 295–307, 2024.

[21] M. Gruenewald, C. Ilies, J. Herz, T. Schoenherr, *et al.*, "Influence of nociceptive stimulation on analgesia nociception index (ani) during propofol–remifentanil anaesthesia," *British Journal of Anaesthesia*, vol. 110, no. 6, pp. 1024–1030, 2013.

[22] M. M. R. F. Struys, C. Vanpeteghem, M. Huiku, K. Uutela, *et al.*, "Changes in a surgical stress index in response to standardized pain stimuli during propofol-remifentanil infusion," *British Journal of Anaesthesia*, vol. 99, no. 3, pp. 359–367, 2007.

[23] J. H. Park *et al.*, "The analgesic potency dose of remifentanil to minimize stress response induced by intubation and measurement uncertainty of surgical pleth index," *Edizioni Minerva Medica*, vol. 84, no. 5, pp. 546–555, 2018.

[24] G. E. Van Poucke, L. J. Bravo, and S. L. Shafer, "Target controlled infusions: targeting the effect site while limiting peak plasma concentration," *IEEE Transactions on Biomedical Engineering*, vol. 51, no. 11, pp. 1869–1875, 2004.

[25] K. Van Heusden, N. West, A. Umedaly, J. M. Ansermino, *et al.*, "Safety, constraints and anti-windup in closed-loop anesthesia," *IFAC Proceedings Volumes*, vol. 47, no. 3, pp. 6569–6574, 2014.

[26] B. Aubouin-Pairault, M. Fiacchini, and T. Dang, "Pid and model predictive control approach for drug dosage in anesthesia during induction: a comparative study," *IFAC-PapersOnLine*, vol. 58, no. 7, pp. 210–215, 2024.